Pergamon

J. Aerosol Sci. Vol. 29, No. 7, pp. 855–874, 1998

Printed in Great Britain
0021-8502/98 $19.00 + 0.00

PII: S0021-8502(97)10013-1

SIMPLIFIED METHOD FOR TESTING PERSONAL INHALABLE AEROSOL SAMPLERS

O. Witschger,*† K. Willeke,*‡ S. A. Grinshpun,* V. Aizenberg,* J. Smith§ and P. A. Baron§

*Aerosol Research and Exposure Assessment Laboratory, Department of Environmental Health, University of Cincinnati, Cincinnati, OH 45267-0056, U.S.A.

§U.S. Department of Health and Human Services, Public Health Service, Centers for Disease Control and Prevention, National Institute for Occupational Safety and Health, 4676 Columbia Parkway, Cincinnati, OH 45226-1998, U.S.A.

(*First received* 22 *May* 1997; *and in final form* 22 *September* 1997)

Abstract—The presently available protocol for evaluating the performance of personal aerosol samplers according to the inhalable convention is difficult to satisfy as it requires a large cross-section wind tunnel. The present study was initiated to simplify and reduce the cost of the test method by mounting the test samplers on a small, stationary torso instead of a full-size rotating manikin. The simplified torso consisted of a rectangular three-dimensional body (33 cm wide, 21 cm deep, 21 cm high). Replicates of the personal inhalable aerosol sampler under consideration were attached in the center of each vertical face of the simplified torso representing the three principal sampling orientations (facing the wind, turned 90°, and turned 180° to the wind). When the samplers were mounted on a full-size manikin, the air flow in the vicinity of the manikin was found to depend on the sampler location, symmetry of the manikin, and position of the manikin's arms. On the simplified torso, the magnitude and direction of the air flow near the samplers were found to be comparable to that of the manikin. When subjected to nearly monodisperse aerosol flows (particle size of 70 μm, wind velocity of 50 and 200 cm s^{-1}), both methods yielded aerosol sampling efficiencies that were statistically not different at three major sampling orientations. The advantages of the simplified torso are that fewer measurements need to be made; a smaller, less expensive wind tunnel can be used for the testing; and interlaboratory variability of personal inhalable samplers' performance may be decreased. © 1998 Elsevier Science Ltd. All rights reserved

INTRODUCTION

Personal aerosol samplers are used for the evaluation of worker exposure to aerosols in occupational environments. Such samplers are usually mounted on the worker's chest and are expected to collect the same concentration of aerosol in the size fraction of interest as the worker inhales, regardless of the particle size distribution, the uniformity of aerosol concentration, and the surrounding air flow pattern. Previous studies have shown that a sampler mounted on a manikin experiences a different flow fields (Rodes *et al*., 1995), and hence collects a different fraction than a free-standing sampler (Buchan *et al*., 1986).

The quantitative descriptions of the different health-related aerosol size fractions in the workplace (i.e. inhalable, thoracic, and respirable) have been standardized by worldwide agreement among the European Standards Organization (Comité Européen de Normalisation, CEN) [EN 481 (CEN, 1993)]; American Conference of Governmental Industrial Hygienists (1996); and the International Organization for Standardization [ISO 7708 (International Organization for Standardization, 1995)]. These conventions specify criteria for commercially available personal and static (or area) aerosol samplers used to assess the possible health effects resulting from the inhalation of aerosols. The performance evaluation of a sampler for the inhalable aerosol fraction (mass fraction of total airborne particles inhaled through the nose or the mouth of humans with average conditions of breathing rates, orientation and external wind speeds) requires laboratory tests using particles up to at least 90 μm and wind speeds of 50 cm s^{-1} and higher (CEN, 1997).

†Author to whom correspondence should be addressed.
‡Present address: Aerosol Physics and Metrology Laboratory, Institute for Nuclear Safety and Protection, DPEA/SERAC, Commissariat à l'Energie Atomique-Saclay, bat 389, F-91191 Gif-sur-Yvette Cedex, France.

Several personal inhalable aerosol samplers have recently been identified by Kenny *et al.* (1997) as candidates for sampling the inhalable fraction: the 37 mm cassette (closed-faced and open-face, SKC Inc., Eighty Four, PA), the CIP10-I sampler (Arelco, Fontenay-Sous-Bois, France), the GSP sampler (Ströhlein GmbH & Co., Kaarst, Germany), the 2 l min^{-1} IOM sampler (SKC Inc., Eighty Four, PA), the PERSPEC aerosol spectrometer (Lavoro e Ambiente, Bologna, Italy), the PAS-6 sampler (produced by the Department of Air Quality, Wageningen Agricultural University, P.O. Box 8129, 6700 EV Wageningen, the Netherlands), and the seven-hole sampler (SKC Inc., Eighty Four, PA, and Casella Ltd., London, U.K.). When using these instruments in workplaces for the measurement of aerosol concentrations, the data from the different samplers may differ from each other significantly since each sampler has its own unique design. Thus, it is important to determine the performance characteristics (bias and accuracy) with respect to the inhalability curve for each of the available samplers. To test sampler performance, the development of an adequate test protocol is essential.

The air flow field around a personal aerosol sampler is influenced by the presence of the human body on which it is mounted. Thus, it is believed that sampler performance evaluations must be conducted with the sampler(s) attached to a full-size manikin simulating the human body (Vincent, 1989). This, in turn, requires a wind tunnel, having a sufficiently large cross-section to fit the manikin and a low blockage ratio, making the evaluation very costly. In addition, wind tunnels which have a large cross-section cannot guarantee sufficient uniformity of the aerosol concentration or air velocity distribution. A recent study of CEN protocols for the performance testing of workplace aerosol sampling instruments (Kenny, 1995) clearly shows the difficulty of testing personal inhalable aerosol samplers in large (e.g. 2 m $\times$ 2 m cross section) wind tunnels. The large variability of the sampling efficiency data obtained for these samplers have been attributed to the non-uniformity of the aerosol concentration. The main recommendation arising from this extensive study is that the time-consuming, expensive, and complex test protocol needs to be simplified and adapted to a smaller wind tunnel. Very few laboratories can afford a large wind tunnel. Thus, improvements of existing inhalable samplers and the development and testing of new ones can be pursued only in a few installations at this time. Among such installations, we can point to a 2.5 m $\times$ 2.5 m cross-sectional area wind tunnel at AEA Technology, Harwell, United Kingdom (Kenny, 1995); a 1.22 m $\times$ 1.83 m wind tunnel at the National Institute for Occupational Safety and Health (NIOSH), Cincinnati, OH (used in this study); a 1.52 m $\times$ 1.22 m wind tunnel at the United States Environmental Protection Agency, Research Triangle Park, NC (Ranade *et al.*, 1990); a 1.6 m $\times$ 1.6 m wind tunnel at the University of California, Los Angeles, CA (Hinds and Kuo, 1995); and a 2.5 m $\times$ 1.5 m wind tunnel at the Institute of Occupational Medicine, Edinburgh, U.K. (Mark and Vincent, 1986).

Previous inhalable sampler studies using manikins have been performed by averaging the sampling efficiencies over 360° rotation. These studies have simulated the possibility of air approaching the worker at random angles and have followed the definition of the inhalable fraction. This was simplified in early experiments by sampling at equal time intervals at each of 45° increments between 0° and 360° (Mark and Vincent, 1986). The results were averaged with equal weight given to measurement at each angle increment. Later experiments used a continuously rotating manikin (Kenny, 1995). Other aspects of the manikin simulating a worker have been also evaluated. For instance, Kenny *et al.* (1997) used "breathing" manikins and found that this approach changed the air flow field at the chest much more than apparently occurred on real workers. Most of the manikin measurements were performed without this "breathing" feature. The flow field around a worker can also be affected by the heat generated by the body. The effect of body heat on the flow field around a manikin has been studied by Johnson *et al.* (1996). The buoyancy of the heated air appears to affect primarily the direction of the downstream flow at low wind velocities, e.g. at 50 cm s^{-1}.

The closer the manikin properties simulate a direction-averaged worker exposure, the more difficult and time-consuming is the testing protocol. The present study was

undertaken to investigate the use of a simplified and cheaper test system and, thereby, to reduce the cost of testing personal inhalable aerosol samplers when compared to the approach taken in recent studies (Kenny, 1995; Hinds and Kuo, 1995). The simplified torso suggested here, the cornerstone of such a system, consists of a rectangular, three-dimensional body having rounded corners. A personal sampler is attached in the center of each vertical face, representing the three principal sampling orientations: facing the wind (0°), turned 90° to the wind, and sampling in the wake of the manikin (180°). Details of body shape, temperature, breathing and angular sampling efficiency are ignored, while attempting to retain the significant effects of body size and orientation on sampling efficiency.

SIMPLIFIED TEST METHOD

Until now, the performance of inhalable aerosol samplers has been evaluated by mounting the samplers on life-size tailor's manikins, as shown in Fig. 1A (Buchan *et al*., 1986; Chung *et al*., 1987; Mark and Vincent, 1986; Mark *et al*., 1994; Vincent and Mark 1990; Kenny *et al*., 1997). In accordance with the inhalable convention, the effects of wind direction are averaged by rotating the manikin continuously or in a stepwise fashion (CEN, 1997). Thus, the aerosol sampler, mounted on the chest of the manikin, passes through the three principal sampling orientations: the body and sampler facing the wind (Fig. 1D), both turned 90° to the wind (Fig. 1G), and both turned 180° to the wind where the sampler operates in the wake of the manikin (Fig. 1D with the sampler attached to the manikin's back).

The new simplified method, developed in the present study, uses a three-dimensional (3D) body (33 cm wide, 21 cm deep, 21 cm high), having rounded corners to simulate the effect of the human body on the sampler, as shown in Fig. 1B. The new simplified method does not utilize an elliptical cylinder (Bull *et al*., 1987; Johnson *et al*., 1996), but simulates the air flow pattern near a full-size manikin with a rectangular body of reduced dimensions. It was designed with rounded corners to minimize undesirable eddies induced by the edges that

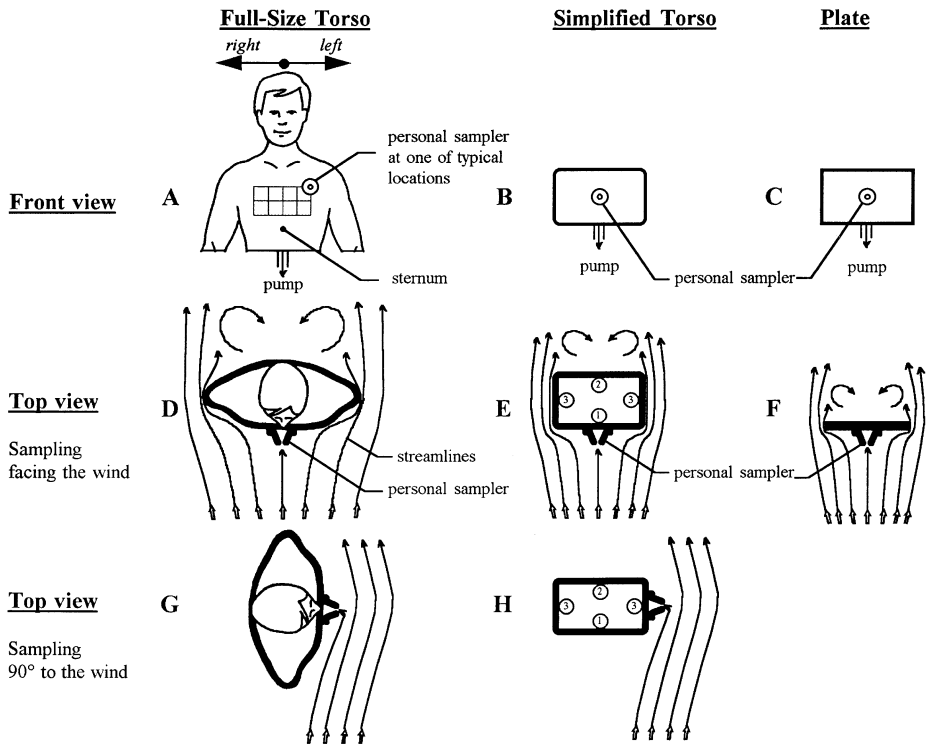

Fig. 1. Test bodies, sampling locations and flow patterns for typical body orientations.

could affect the flow pattern on each side of the body. The new 3D body allowed reducing the number of experiments so that the aerosol sampler under investigation was tested without rotation in all three principal orientations (0, 90°, and 180°) during each test at specified aerosol and wind conditions. Thus, a sampler was mounted on each vertical face of the simplified torso, each representing one of the sampling orientations (Fig. 1E and H): position 1 represented the sampler and human body facing the wind, position 2 represented the body and sampler turned 180° to the wind, and position 3 represented the body and sampler turned 90° to the wind. When a worker wears a personal aerosol sampler, the sampler is mounted on the worker's chest, usually in the breathing zone (ACGIH, 1995), but no specific location is indicated. Different locations are used in practice for different types of samplers (within the area defined by the grid in Fig. 1A). When testing in accordance with the simplified method, each sampler was located in the center of each vertical surface of the simplified torso, Fig. 1E and H.

A personal sampler is often operated facing the wind (Fig. 1D). Thus, the sampler evaluation usually begins with testing at this specific orientation. In order to determine whether the new test method proposed in this study could be further simplified utilizing a 2D body (for the situation when the body and the sampler face the wind), a thin rectangular plate was also tested, as shown in Fig. 1C and F. The plate had the same dimensions as the front face of the 3D simplified torso, i.e. 33 cm wide and 21 cm high.

EXPERIMENTAL SETUP AND PROCEDURES

The laboratory evaluation of the simplified test method was conducted in two parts. The first part was an air flow study in which air flow visualization and air velocity measurements at 0°, 90°, and 180° were carried out around all three test bodies (full-size torso, simplified torso, and flat plate). In the second part, the particle sampling efficiencies were determined in all three sampling orientations for a commercially available personal inhalable aerosol sampler mounted on either the full-size torso or the simplified torso.

Wind tunnel

The tests were performed in a large cross-section, closed-loop wind tunnel located at NIOSH in Cincinnati, OH. Figure 2 shows a top view of the working zone of the wind tunnel and the two experimental configurations described below. The working section was 1.22 m high and 1.83 m wide. The air velocity could be varied from 30 to 300 cm s^{-1} covering typical air velocities encountered in indoor working environments (Berry and Froude, 1989). The air was moved through the facility by a centrifugal fan and drawn through a filtration unit (including HEPA filters), located upstream of the working zone. This arrangement provided clean air to the working zone and also removed large scale turbulence produced upstream of the filter. To further ensure a uniform spatial distribution of the air flow, a flow straightener (honeycomb) was located upstream of the working zone. This also induced an isotropic and homogeneous turbulence region. The air velocity in the working zone was found to be uniform within $\pm$ 5%, and the turbulence intensity was measured to be less than 6% for both test air velocities of 50 and 200 cm s^{-1}. The lateral and vertical free stream air velocity components were measured to be less than 5 cm s^{-1}, i.e. the main flow was parallel to the centerline of the wind tunnel.

The working zone was physically and optically accessed through the two removable acrylic windows (1 m $\times$ 1 m each) on either side of the wind tunnel. The full-size torso and the simplified bodies (two-dimensional plate and three-dimensional simplified torso) were placed on the centerline of the tunnel about 2 m downstream of the flow straightener, as shown in Fig. 2. Table 1 shows that the blockage by the full-size torso was 16% or less. The blockage was only 3% for the simplified bodies. Thus, the air flow around the test bodies was not substantially affected by the presence of the tunnel walls. The simplified test bodies were mounted on a stand; thus, each aerosol sampler was located at the same height and was exposed to the same free stream air flow and aerosol concentration. The

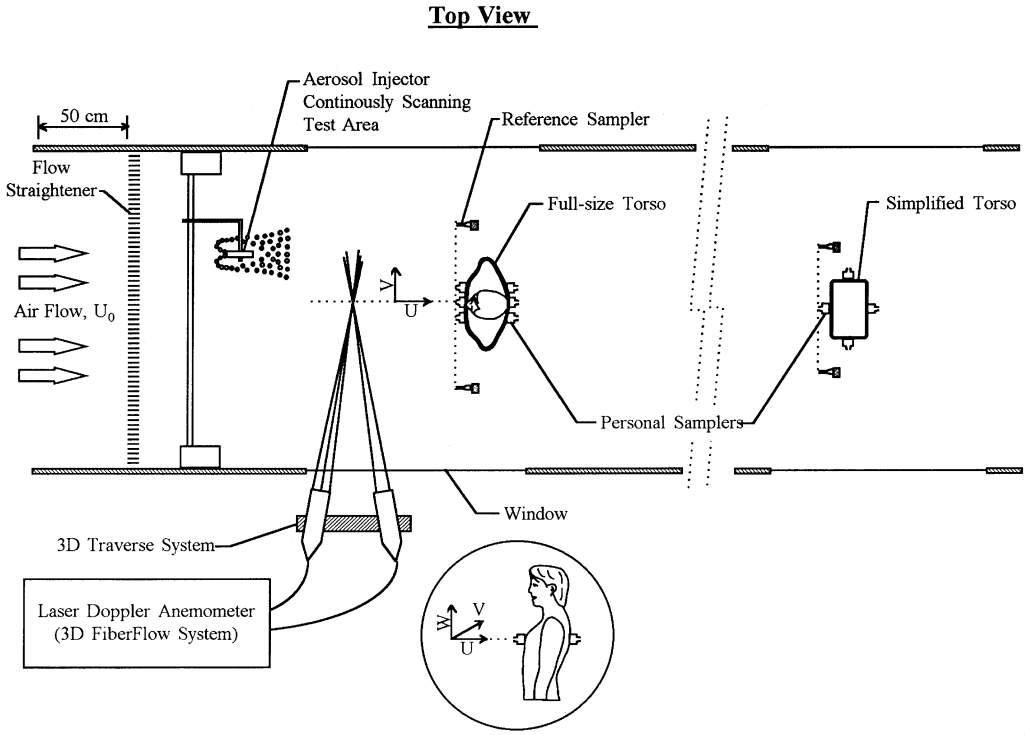

Fig. 2. Schematic diagram of the experimental setup for air flow and aerosol sampling efficiency measurements.

Table 1. Characteristics of the test bodies

	Full-size torso	Simplified torso	Plate
Width (cm)	50 (Shoulder level)	33	33
Height (cm)	81	21	21
Depth (cm)	21 (Chest level)	21	0.5
Blockage[a] (%)	16 (Facing wind) 8 (90° to wind)	3	3

[a] Blockage is relative to the wind tunnel working section (183 cm wide × 122 cm high)

manikin and the simplified test bodies were coated with graphite paint to make them conductive.

The influence of these torsos on the air flow around a personal aerosol sampler has been studied using two commercially available inhalable aerosol samplers: the IOM 2 l min^{-1} personal aerosol sampler and the GSP 3.5 l min^{-1} personal aerosol sampler (Vincent, 1989; Kenny *et al.*, 1997). These samplers were chosen because both have a centrally located circular inlet, but they differed by the distance of the inlet face from the base of the sampler, 2.8 cm for the IOM and 7.5 cm for the GSP (sampler holder included). The GSP was chosen for the particle efficiency measurements. While this sampler did not provide the best match with the inhalability convention, it was ranked highest in precision according to a European study (Kenny *et al.*, 1997) among 8 tested personal inhalable aerosol samplers.

Flow visualization and velocity measurements

Smoke streamlines used to visualize the flow pattern (streamlines and vortices) near a body can be very informative, especially if the flow is relatively complex. This technique was applied to the three test bodies (full-size torso, the simplified 3D torso and 2D plate) in

order to qualitatively evaluate the flow patterns for the different sampling orientations. Fine streams of smoke were isokinetically injected at different points of interest all around the test bodies providing local streamline analysis. The generation of a uniform dense cloud by a theatrical smoke generator (Rosco Inc., Port Chester, NY) aided the study of the main flow around the test bodies. In order to quantitatively describe the flow pattern and compare the results among the three test bodies, air velocity measurements were performed using a laser Doppler anemometer (LDA, 3D FiberFlow System, Dantec Electronics Inc., MahWah, NJ). The LDA technique had several advantages over the hot-wire anemometer technique: it was non-intrusive, did not require calibration, was relatively easy to set up and align, and allowed three-dimensional velocity measurements when used with appropriate multi-component probes. The LDA, see Fig. 2, was located outside the wind tunnel on a high precision 3D motor traversing system (Dantec Electronics Inc.), which provided an accurate spatial reference of the measurement points and facilitated data acquisition relative to a pre-determined 3D mesh.

The air flow in the working zone was seeded with an oil droplet aerosol (food-grade corn oil), which was generated by a custom-made nebulizer. Measurements using an Aerodynamic Particle Sizer (APS 33, TSI Inc., St. Paul, MN) indicated a number median aerodynamic diameter of the liquid droplets of 0.7 μm, having a geometric standard deviation, σ_g, of 1.3. At this and smaller particle sizes, the influence of particle inertia was negligible, i.e. the droplet trajectories essentially followed the air streamlines.

The first velocity measurements were performed in front of the manikin's chest, i.e. for the 0° sampling regime, at locations that were 5, 10, 15, 20, 25 or 30 cm upstream of the manikin. The measurement points were defined by the 20 cm wide and 10 cm high grid shown in Fig. 1A. The 15 grid points in each plane were 5 cm apart from each other. Thus, 6 grid planes, having 15 points per grid, resulted in 90 measurement points. That allowed the determination of flow deceleration in front of the body along different lines relative to the central location of the aerosol sampler. The lowest grid line was located 5 cm above the sternum level. Thus, the distance between each grid points and the mouth was less than 30 cm. This distance allowed the personal sampler to be within the area defined as the "breathing zone" (ACGIH, 1995). When sampling with the manikin turned 90° or 180° to the free stream air velocity, measurements were performed only along the centerline, projecting outward from the grid. When the three-dimensional simplified torso was studied, the air velocities were measured along the centerlines projecting outward from the front, side, and rear faces of the body. The air velocity along the centerline of the flat plate at 0° was also measured. Measurements were performed with and without the personal aerosol samplers attached to the bodies. When the IOM or GSP sampler was attached to the body, the sampler's inlet was aligned with the centerline, along which velocity measurements were made. The two samplers were operated at their respective flow rates of 2 and 3.5 l min^{-1}. The flow measurements were made at a distance of 5 and 7.5 cm from the chest when the IOM and GSP samplers, respectively, were in place because the LDA had difficulty with beam blockage at smaller distances from the body.

Aerosol sampling efficiency measurements

The second part of this laboratory study evaluated whether a personal inhalable aerosol sampler had similar performance (aerosol sampling efficiency) while mounted on the full-size versus the simplified torso. Only the GSP sampler, operated at 3.5 l min^{-1} (Kenny, 1995; Kenny *et al.*, 1997), was selected to test the above hypothesis. The aerosol sampling efficiency, E_S, of the GSP was determined as the ratio of aerosol mass concentration, measured by the GSP, to the average of aerosol mass concentrations, measured by two reference samplers that were mounted adjacent to the manikin, as shown in Fig. 2. The reference samplers were mounted in the free stream, at a lateral distance of 43 cm from the middle GSP sampler that was attached to the manikin. The reference samplers were located at the same height and distance from the aerosol injector as the GSP samplers. At these locations no change was observed in the air streamlines that could have resulted from the

presence of the torso and personal aerosol samplers. Thus, the reference aerosol concentration was defined as the free stream aerosol concentration and, therefore, it was not affected by the presence of the test bodies. The mass concentration of the GSP was determined by gravimetric analysis of its 37 mm glass fiber filter. The reference aerosol concentration was determined by isokinetic sampling on 25 mm glass fiber filters. Each reference probe had a 10 mm diameter inlet made of an 80 mm long thin-walled tube, meeting the Belyaev and Levin (1974) criteria. The particles deposited on the walls inside the reference probes were carefully removed by a washing technique (Witschger *et al*., 1997) and collected on 25 mm membrane (PVC) filters. The total particle mass collected by the filter and washed from the walls determined the reference concentration.

A key feature of the wind tunnel is the aerosol generation system. The aerosol was generated by a powder disperser (model RBG-1000, Palas GmbH, Karlsruhe, Germany) whose output is a constant, continuous, and reproducible aerosol concentration. Nearly monodisperse aluminum oxide particles (Fusco Abrasive Inc., Compton, CA), with a mass median aerodynamic diameter of 70 μm and a geometric standard deviation of 1.35, were used as the test aerosol. A sedigraph (Model 5000 Sedigraph, Micromeritics Instrument Corp., Norcross, GA) was used to measure the particle size distribution of the alumina powder. To derive the aerodynamic diameter from the sedimentation analysis, a density correction was made, but no dynamic shape factor was introduced. Only one particle size was used in this study because of time and expense constraints. However, the sampling efficiency of a personal inhalable aerosol sampler, such as the GSP sampler, changes relatively little with the particle size in the large size range (Kenny *et al*., 1997), and the particle size of 70 μm is representative of that range. The test generator output was exposed to a high concentration of bipolar ions, produced by an AC corona discharge, in an air flow controller (model AFC-2, Richmond Static Control Services Inc., Palm Springs, CA). The charge-neutralized particles were injected into the wind tunnel through an injection tube in the direction opposite to the main flow direction, as shown in Fig. 2. This configuration prevents particles from being directly projected into the sampler by the injection system, and assures that all agglomerates settle out of the test region by gravitational sedimentation. Tests with the aerosol injection tube at a fixed location showed that the vertical and horizontal dimensions of the aerosol plume in the sampling zone were 50 cm wide in all directions. The aerosol injection tube was mounted on a traverse system, driven by a stepping motor, so that it continuously scanned the test area.

Each sampling experiment consisted of traversing a 127 cm wide area four times, resulting in a minimum 3 h sampling duration. Each horizontal scan was at a 3.81 cm vertical distance from the previous scan. Very good spatial uniformity of the aerosol concentration and reproducibility between runs was achieved using this method. The coefficients of variation for spatial uniformity and the reproducibility between runs were less than 0.04 for the reference concentration when tested at the air velocity of 50 cm s^{-1}. They were less than 0.02 for the air velocity of 200 cm s^{-1}. The average mass concentrations in the test section at the two air velocities were 10 and 4 mg m^{-3}, respectively. The mass concentration was determined by gravimetric analysis using an analytical balance (model AT20, Mettler Toledo Inc., Hightstown, NJ) at a temperature of 23°C and relative humidity of $60 \pm 10\%$. Samples were equilibrated under these conditions for at least one hour prior to weighing. The limit of detection (LOD) and limit of quantitation (LOQ) for the mass of collected filter deposits were estimated from the standard deviation, σ, of a set of measurements with blank filters that were handled the same way as normal samples. The mass of typical filter deposits ranged from 0.04 to 1.55 mg depending on the sampling orientation and free stream velocity. The LOD was calculated to be $3\sigma = 64$ μg per sample and the LOQ to be $10\sigma = 214$ μg per sample (Kennedy *et al*., 1995). All measurement values for samples taken at 0° and 180° were above the LOQ; 53% of the measurements for 90° sampling were between the LOD and LOQ, and the rest were above the LOQ. The measurements at 90° may thus have had somewhat greater variability associated with them due to analytical error. Values of the sampling efficiency that were derived from the gravimetric measurements of filter deposits were accepted if they were higher than its limit of detection, LOD.

When tested on the full-size torso, three GSP samplers were attached to the chest of the manikin and three to its back, as shown in Fig. 2. The positions of the three samplers in the front and back were at the locations R10, C, and L10 at level H5 defined in Fig. 3. Thus, one sampler was located at the center (C) of the grid at a height $H = 5$ cm above the baseline (H0) of the grid. The other two samplers were located at the same height, at distance $R = 10$ cm to the right, and distance $L = 10$ cm to the left of the central sampler. The 10 cm separation distance avoided interactions between the samplers. When the full-size torso was positioned facing the oncoming air flow in the wind tunnel, the three samplers on the chest determined the mean aerosol sampling efficiencies for the 0° sampling regime, while the three in the back determined the mean aerosol sampling efficiencies for the 180° sampling regime. For the 90° sampling regime, the manikin was turned 90° to the wind tunnel air flow. In the latter configuration, six samplers oriented perpendicular to the air flow (three on the chest and three on the back of the manikin) determined the mean aerosol sampling efficiency.

When tests used the simplified 3D torso, only one sampler was attached to each vertical face, as shown in Fig. 2. The sampling efficiency data from the samplers in the front and the

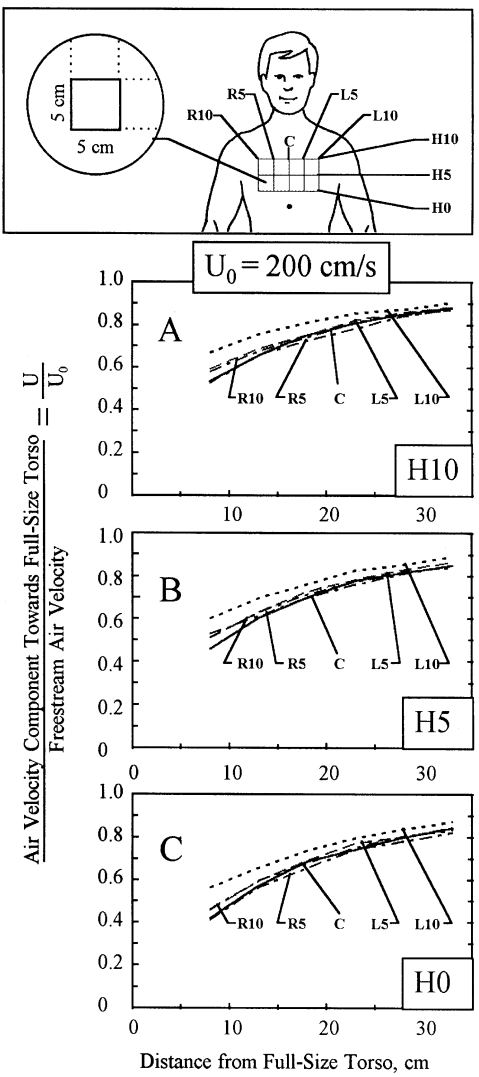

Fig. 3. Normalized air velocity component towards the chest of the full-size torso when facing the wind. Free stream air velocity = 200 cm s^{-1}. No personal aerosol sampler was mounted on the manikin's chest during these measurements.

back corresponded to the 0° and 180° regimes, respectively. The sampling efficiencies of the samplers located on each side were averaged and attributed to the 90° sampling regime. Thus, only one experiment was needed to obtain data for all three sampling regimes using the simplified body, whereas two experiments had to be conducted when the full-size torso was used. For each sampling position, a GSP sampler was chosen randomly to avoid systematic errors in data acquisition. The experiments were performed in random order and each condition was tested at least three times.

RESULTS AND DISCUSSIONS

Flow visualization and velocity measurements

Figure 3 shows the horizontal air velocity component, U, towards the full-size torso facing the wind. This air velocity component is parallel to the free stream air flow and is non-dimensionalized relative to the free stream air velocity. The latter was 200 cm s^{-1} for all of the data shown in Fig. 3. Each curve is the result of measurements made at the grid points shown in the top diagram of Fig. 3. The centerline for all the measurements (C, H5) is located about 10 cm above the manikin's sternum and about 20 cm below the mouth. The curves in this figure indicate that the air flow starts to decelerate at about 30 to 35 cm from the manikin. As the air moves towards the manikin, flow blockage by the manikin increases the hydrostatic pressure on the manikin's chest. As a result, the air flow moves in the direction of decreasing pressure: primarily in the horizontal direction away from the chest and, to a lesser degree, upward toward the shoulders. Rodes *et al.* (1995) observed similar flow patterns. Figure 3B shows that the air velocity at 7.5 cm from the chest, corresponding to the inlet face of the GSP sampler, is 45 to 60% of the free stream air velocity. Figure 3 also shows that U at heights H0 and H5 is lower than at height H10 because the air flow is deflected toward the manikin's shoulders, which creates higher air velocities at height H10. This air flow deflection was also observed through smoke streamlines. The air velocities toward the chest at different lateral positions differed by only 15% or less of the free stream velocity. The measured air velocities at the left end on the grid, L10, were somewhat higher than those at the right end of the grid, R10. This is explained by the slight asymmetry of the manikin used in this study. The manikin leaned to its left side allowing the flow to pass more easily over the shoulder on this side, thus, reducing the flow deceleration.

Figure 3 shows that there is no typical deceleration curve upstream of the manikin's chest. The flow deceleration depends on the location where the personal aerosol sampler is placed on the body. While submicrometer-size particles tend to closely follow the motion of the air, large particles, such as 50 to 100 μm diameter particles, have appreciable inertia and gravitational settling velocity, and may, therefore, deviate from the air streamlines. This implies that the performance of an inhalable personal aerosol sampler depends on the sampler's location on the chest. Previous tests using personal inhalable aerosol samplers, such as those by Kenny *et al.* (1997), have not reached this conclusion, probably because the considerable spread of their data hid these smaller biases.

Figure 4 shows the influence of the physical shape and the inlet flow on the air velocity toward the GSP (Fig. 4A) and IOM (Fig. 4B) samplers when tested at free stream air velocities of 50 and 200 cm s^{-1}. U_i represents inlet velocities of 116 and 19 cm s^{-1} for the GSP and IOM samplers, respectively. The air velocity measurements were performed on the centerline (C, H5) of the manikin, with and without a sampler. For each of the free stream air velocities, the air flow toward the body was not significantly affected by the physical size or inlet flow of either sampler. However, the air velocity near the inlet face of the GSP sampler, located at 7.5 cm from the body, was about 40% of the free stream air velocity, while it was only about 30% near the face of the IOM sampler, located at 2.8 cm from the body. Thus, the height of a personal aerosol sampler may influence the performance of the sampler, as suggested in a theoretical investigation by Ingham and Yan (1994).

Figure 5 shows the flow deceleration along the centerlines of the two smaller test bodies, i.e. the simplified torso and the plate, shown in the upper part of the figure. The error bars

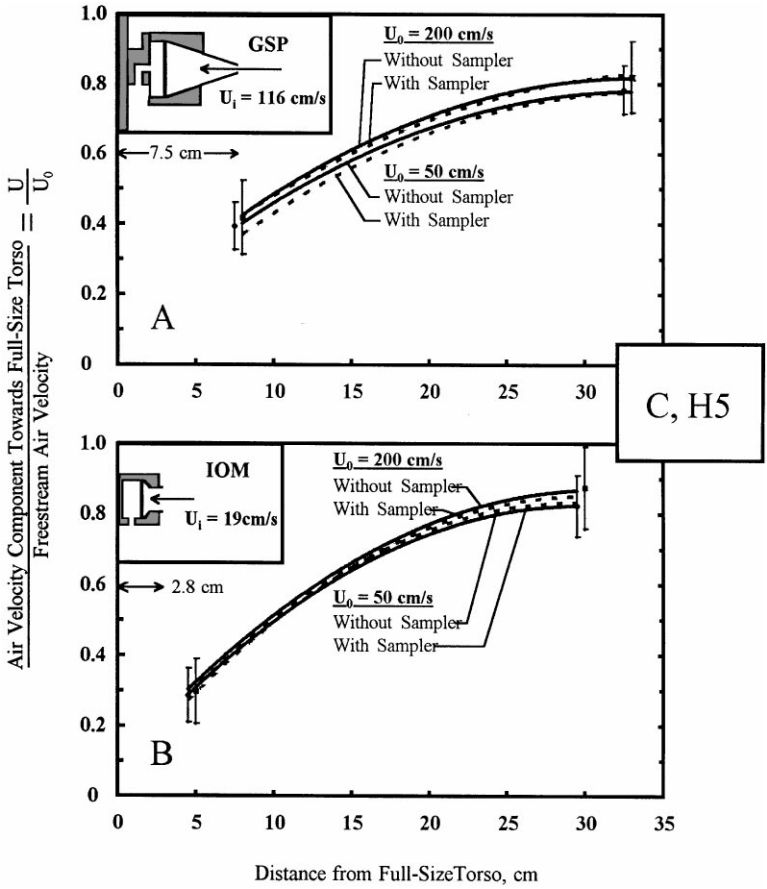

Fig. 4. Normalized air velocity component towards full-size torso, facing the wind, used with and without an operating sampler. Free stream air velocities = 50 and 200 cm s^{-1}. The GSP sampler was operated at 3.5 l min^{-1}, the IOM sampler at 2 l min^{-1}.

represent 95% confidence intervals. The dotted lines are the highest and lowest deceleration curves measured within the grid of the full-size torso (from Fig. 3). To achieve comparable aerosol sampling conditions, the flow deceleration curves for the smaller bodies should be mostly within these dotted curves. As seen, the deceleration curves for smaller test bodies do fall within the limits of the air flow deceleration curves for the manikin, starting at about 15 cm distance from the bodies and closer.

The air flow deceleration toward these smaller test bodies was about the same for both free stream air velocities, 200 cm s^{-1} (Fig. 5A) and 50 cm s^{-1} (Fig. 5B), as also observed for the full-size torso (Fig. 4). Smoke streamlines observations on the chest of the manikin showed that some air flow passed through the space between the arms and the body. The body width of the simplified torso was chosen to be 33 cm, less than the 36 cm width of the full-size torso without arms. The smaller width of the simplified torso yielded air flow deceleration curves similar to those of the full-size torso, apparently because the latter was a convex body while the former was flat. The slight difference in the curves between the plate and the simplified torso may be attributed to the rounded corners of the simplified torso.

Since the flow around a full-size manikin was three dimensional, we also investigated the lateral and vertical components of the flow in the chest area. Figure 6 shows the lateral air velocity component, V, in front of the test bodies. The measurements in front of the manikin were performed using the grid defined in Fig. 3. It can be seen that the lateral velocity component was a strong function of the position relative to the stagnation point (where all velocity components are zero). The stagnation point ($V = 0$) was located between the two vertical lines C and R5 (see grid definition in Fig. 3), i.e. it was displaced by less than 5 cm to

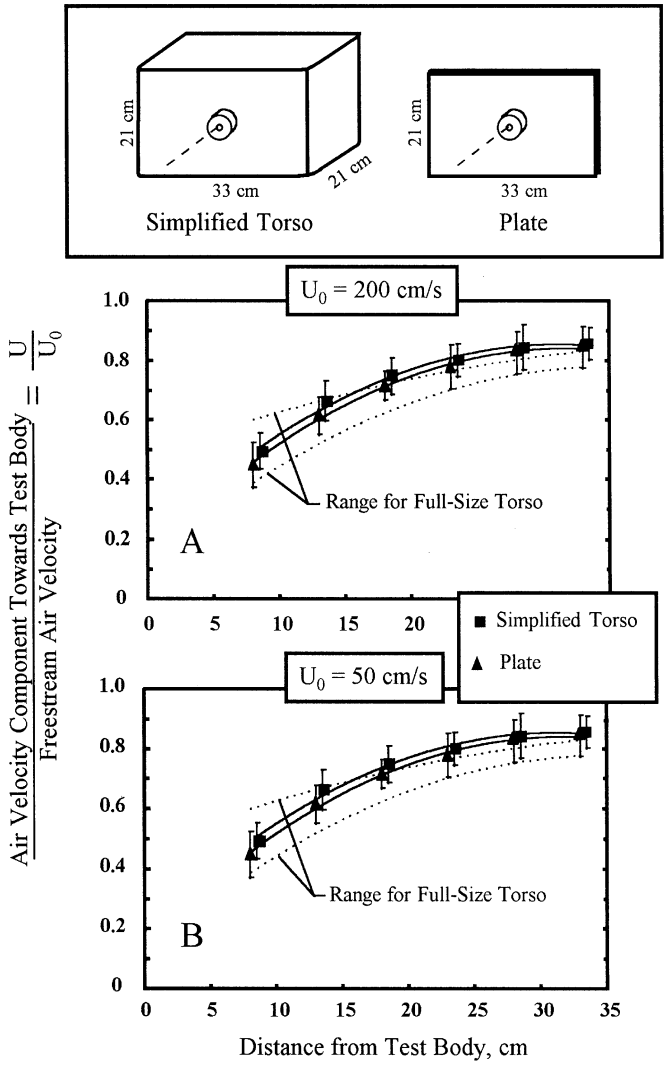

Fig. 5. Normalized air velocity component towards test torsos. Error bars represent the 95% confidence interval on the measured data.

the right from the body's geometric center. The previously mentioned slight leaning of the manikin to the left allowed more air flow to pass by the left side of the body, thus, shifting the stagnation point to the right of the body's geometric center. Consequently, the lateral air velocity component should be highest at the greatest distance from the stagnation point. Figure 6A shows this to be true for vertical line L10 close to the shoulder, H10.

The above air velocity measurements show that the air flow approaching a full-size torso is complex. The air velocity deceleration curves upstream of the sampling point appeared to be dependent on the location of a personal sampler on the chest of the manikin in the breathing zone. These curves may also be affected by a torso's size and design. Thus, a much wider range of air flow patterns is likely to be found near the chest of workers of different body size and build. It was, therefore, decided that the simplified torsos should produce an approaching flow having air velocity components within the range of air velocity measured on the full-size torso. The smaller test bodies were designed to have an essentially zero lateral velocity component at their geometric center where the test personal aerosol sampler was placed. As different locations on the worker's chest are used for different personal samplers, the testing procedure developed in this study did not include such a positioning factor. Thus, by locating the tested personal sampler at the center of each vertical face, the

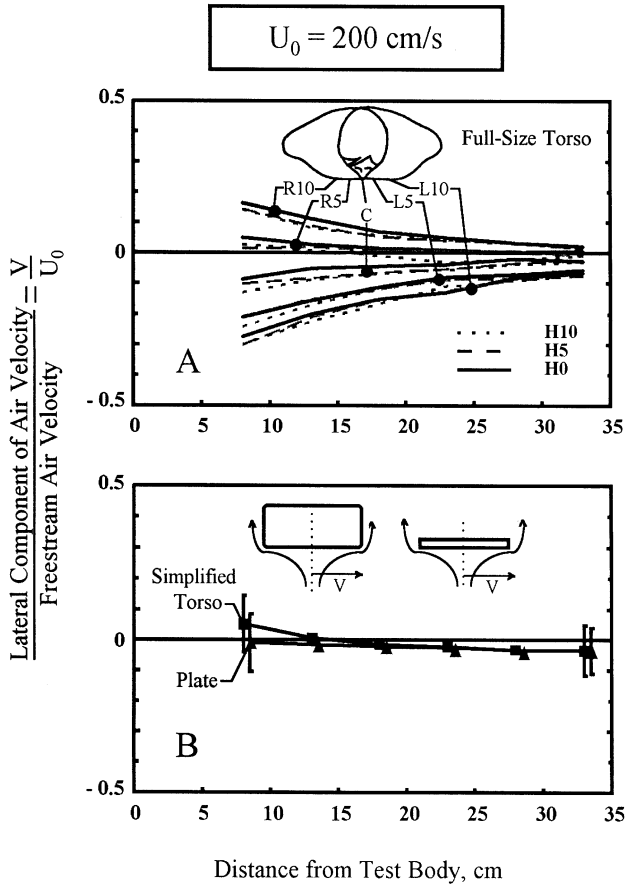

Fig. 6. Normalized lateral component of air velocity for the test bodies facing the wind.

same wind and aerosol conditions were assured in each test. This location also minimizes the edge effects that could modify the air flow approaching the sampler. The positioning is shown in Fig. 6B for the simplified torso and the plate.

Measurements of the vertical air velocity component, *W*, along the centerline (C, H5) were performed on a full-size torso having the arms in different extreme positions: forearms reaching forward, Fig. 7A; arms hanging down, Fig. 7B; and arms stretched upward, Fig. 7C. When the arms were pressed against the body and the forearms reached forward, some of the air flow easily moved upward over the shoulder, as seen by the uppermost curve in Fig. 7. When the arms hung down, there was a small upward air velocity component. When the arms were stretched upward, however, the vertical component essentially disappeared. Thus, the air flow close to the chest is also a function of arm position. This suggests that the vertical dimension for the smaller test bodies was not a critical parameter. Figure 7 shows that the vertical air velocity components at the center of the simplified torso and the plate were essentially zero. With the LDA laser beam system as set up in Fig. 1, it was not possible to investigate the air flow closer to the chest than indicated in Figs 3–8. Smoke observations indicated that a mixing layer existed within a few centimeters of the body. The thickness of the mixing layer appears to be about the same for both tested free stream air velocities of 50 and 200 cm s^{-1}.

The second part of the air flow comparison between the full-size torso and the smaller test bodies was performed in the 90° sampling regime. The manikin was turned 90° to the direction of the free stream flow axis, as shown in Fig. 1G. The simplified torso was not turned. Instead, the personal aerosol samplers were placed on the sides of the simplified torso located at positions 3, Fig. 1H. As seen, the horizontal air velocities parallel to the

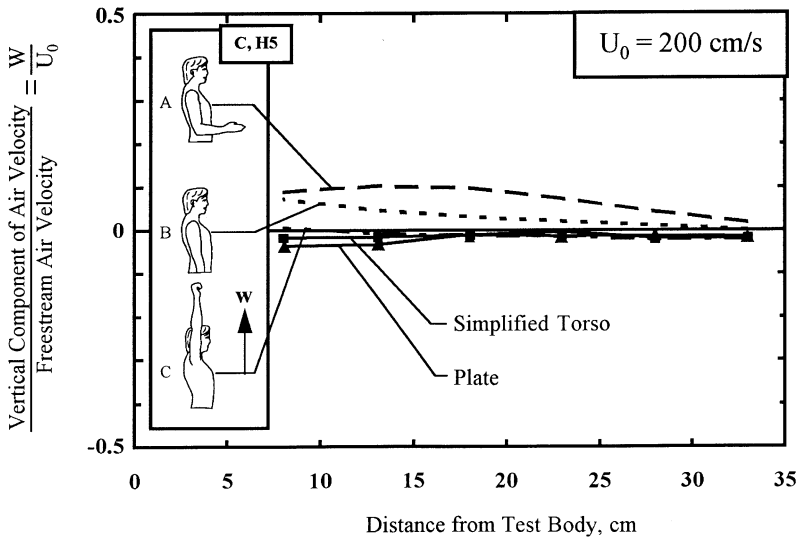

Fig. 7. Vertical components of air velocity. The full-size torso has three different arm positions: A: Forearms reaching forward. B: Arms hanging down. C: Arms stretched upward.

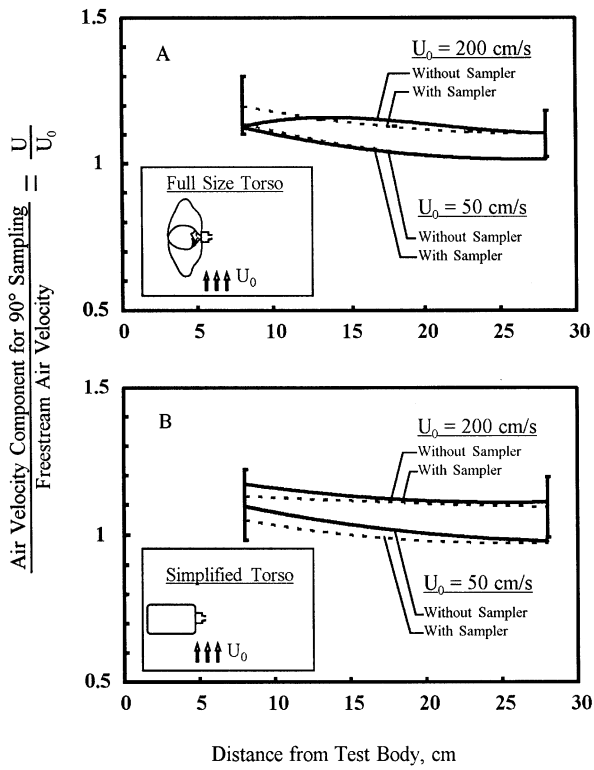

Fig. 8. Air velocity component in the direction of the main flow when the test bodies are at 90° to the wind. Test were performed with the GSP personal aerosol sampler operated at 3.5 l min^{-1}

wind tunnel axis were essentially the same for the full-size torso, Fig. 8A, and the simplified torso, Fig. 8B. The acceleration levels were somewhat higher for the 200 cm s^{-1} than for the 50 cm s^{-1} free stream velocities in the presence of either of those bodies. When the GSP sampler was placed and operated on those bodies, as shown in Fig. 8, the air velocities were not significantly affected. Similar conclusions were drawn from smoke streamline

visualization studies that resulted in the sketches of the flow patterns shown in Fig. 1G and H.

A conclusion was also drawn from Fig. 8 regarding the placement of the reference samplers (Fig. 2). Figure 8 shows that the difference between the air velocities 20 cm from the side of the full-size or simplified torso and the free stream air velocity did not exceed 15%. Thus, the reference samplers, located at this distance from each side of the test bodies (both the full-size and simplified torsos), took approximately isokinetic samples.

When a bluff body, such as a manikin, is turned 180° to the wind tunnel air flow, a boundary layer separates from the body as the flow moves around the side of the body, and produces a wake similar to that which is classically observed behind a circular cylinder positioned in a uniform free stream (Schlichting, 1979). Separation occurs when the air motion in the boundary layer around the body encounters an adverse pressure gradient. This phenomenon is of interest in worker exposure because it can transport contaminants into the breathing zone of a worker turned 180° to the main air flow (Flynn and Ljungqvist, 1995; Flynn *et al*., 1995). Overall, the nature of air flow around a personal aerosol sampler attached to a bluff body is rather complex and may significantly affect the performance characteristics of the sampler (Sreenath *et al*., 1997).

Our flow visualization studies showed that the air flow pattern behind the manikin and the simplified torso was dominated by the shedding of vortices and the presence of turbulent motion. By introducing smoke on each side of the test bodies at the sampler location level, it was possible to visualize the shedding of the vortices. We estimated the average width of the vortices to be equal to half of the test body's width (16.5 and 18 cm for the simplified and full-size torsos, respectively). For both test bodies, the vortex widths were about the same for both tested free stream air velocities, 50 and 200 cm s^{-1}. Our vortex observations were consistent with the vortex dimensions given by Kim and Flynn (1991). Thus, it is believed that the flow pattern behind the simplified torso is similar to the one near the front of the full-size torso when it is turned 180° to the flow.

The flow pattern near the inlet of a personal aerosol sampler mounted on a full-size manikin (flow separation, occurrence of vortices, spatial dependence of the flow field, etc.) depends not only on the sampler location on the torso or on the orientation of the torso but also on the manikin's size, shape, and arrangement of the torso's extremities, such as the arms (see Fig. 7). These factors possess a natural variability resulting from the variety of manikin models offered by different manufacturers over the years. Since every laboratory that has published performance data used a different manikin, each having its own unique arm positions, loss of precision and an interlaboratory bias were likely to occur. The simplified 3D torso having a personal aerosol sampler placed in specified locations representing all three major wind directions, would significantly reduce this source of interlaboratory bias.

The air measurement near a human being may also be influenced by other effects, such as breathing or free convection caused by the metabolic heat of the human. Wood and Birkett (1979) found that exhalation induced a downdraft to the chest, but the performance of personal aerosol samplers was not noticeably affected when sampling was performed using the manikin facing the air flow. In a recent study Johnson *et al*. (1996) compared the air flows in the wake of a tailor's manikin with those in the wake of a human. They found that thermal effects dominate over breathing effects in the air flow near the body when the free stream air flow is very low.

Figures 5–8 show that the air flows at the 0°, 90°, and 180° aerosol sampling locations of a simplified torso were within the range of air flows at comparable locations and orientations of a full-size manikin. This suggests that the aerosol particle trajectories approaching the test bodies should be comparable as well, resulting in equivalent aerosol sampling efficiencies.

Aerosol sampling efficiency measurements

Figure 9 compares the aerosol sampling efficiencies of the GSP samplers when mounted on the full-size manikin versus the simplified torso for the three sampler orientations (0°, 90°

and 180°), at two air velocities (50 and 200 cm s^{-1}) and the particle aerodynamic diameter of 70 μm. The vertical bars represent the 95% confidence of the mean sampling efficiency calculated from at least three experiments for each sampling regime. For the 0° and 180° orientations, the data points for the full-size manikin were obtained by averaging the data from the three GSP samplers and then averaging the three repeats. The data points for the simplified torso represent the values from one GSP sampler averaged over three repeat experiments. For the 90° sampling regime, the data obtained with six samplers were averaged for the full-size manikin (three on the chest and three on the back, all of them orientated perpendicular to the wind direction). For the simplified 3D torso oriented at 90°, the data obtained with two samplers were averaged (one sampler on each side perpendicular to the wind). The data show that the sampling efficiency values obtained using the simulated torso were within the range of those obtained using the full-size manikin.

Figure 9 also shows that the sampling efficiency drops considerably when the sampling orientation changes from the isoaxial one. This drop can be explained by the sensitivity of the sampling efficiency of the GSP sampler to changes in the free stream air velocity and sampler orientation. This allows us to make two conclusions: First, in the development of a personal aerosol sampler, the sampler's dependence on free stream air direction and velocity should be minimized. The second conclusion concerns averaging of the sampling efficiencies over all wind directions. It is common to assume that all of the available personal samplers intended to collect the inhalable fractions are wind-direction dependent when mounted on a body. Hence, it is important to know their typical performance for the major sampling regime orientations. These types of experiments can more easily be conducted using the simplified testing technique developed in this study.

An analysis was performed to determine if a statistically significant difference exists between the results obtained by use of the full-size versus the simplified torso. The *t*-test for these two populations having non-equal variances was performed for each sampling orientation. The difference between the mean values of the sampling efficiencies was

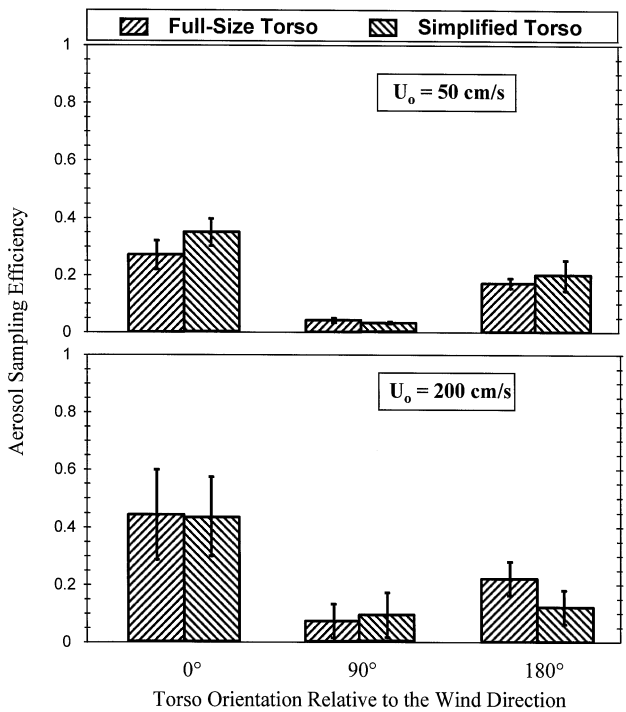

Fig. 9. Comparison of the particle sampling efficiencies measured with GSP samplers mounted on full-size and simplified torsos; tested at three sampling orientations: facing the wind (0°), turned 90° to the wind, turned 180° to the wind. Sampling flow rate = 3.5 l min^{-1}, particle aerodynamic diameter = 70 μm.

analyzed, as described by Smith (1938) and Satterthwaite (1946). When the calculated t values fell inside the interval $[-t_{0.975}; t_{0.975}]$ for the sample degree of freedom, df, the means of the sampling efficiencies of the GSP sampler measured on the full-size versus simplified torso were judged not to be significantly different at the 5% confidence level ($p < 0.05$). Table 2 presents the results of the statistical analysis of the experimental data. As was indicated above, each full-size torso experiment yielded three efficiency values, while each experiment using the simplified torso yielded only one efficiency value (see also Fig. 2). In addition, the 95% confidence intervals on the difference between the mean aerosol sampling efficiencies of the GSP sampler mounted on the full-size versus the simplified torso were calculated for each orientation. The t-tests and the 95% confidence intervals demonstrate that there is no statistically significant difference in the sampler performance when tested on the full-size and the simplified torso. This holds true for both wind velocities (50 and 200 cm s^{-1}), for all three sampling orientations (0°, 90°, and 180° to the wind), when sampling particles of 70 μm in aerodynamic diameter with the GSP sampler. These data support the use of the simplified torso for wind tunnel testing of personal inhalable aerosol samplers.

Some intersample variability was noticed in our experiments. Despite the fact that the dust generator may have produced additional turbulence at the sampling point, the intersample variability cannot be attributed to the generation system alone because it was found that the reference isokinetic samplers demonstrated very good precision (the average coefficient of variation for the reference isokinetic samples was below 1%). At the same time, particle deposition was observed between the inlet and the filter of the GSP samplers, particularly on the rim of the filter holder. These internal losses, that primarily occurred on the filter holder's rim, were found to be 48% of the mass aspirated through the GSP entry orifice when the wind velocity was 50 cm s^{-1}. At 200 cm s^{-1}, the losses were about 33%. However, since it is a common practice in field aerosol sampling to assume no transmission losses, only the filter deposits were used in determining the aerosol sampling efficiency of the GSP samplers. While it cannot be concluded from the collected data that the simplified torso yields more precise results than the manikin, we expect that separate studies using different aerosol samplers will confirm our prediction of better data precision from the simplified torso approach.

To compare the results from the simplified torso with a manikin rotating a full 360°, a weighted average can be used: $E_{\mathrm{TOTAL}} = (aE_0 + bE_{90} + cE_{180})$, where the weighting factors for a simple average are $a = 0.25$, $b = 0.50$, and $c = 0.25$. These factors represent, respectively, the relative time contributions of the three primary sampling orientations. Using this weighting scheme, the average efficiency of the GSP sampler at 70 μm was 0.15 at 50 cm s^{-1} and 0.18 at 200 cm s^{-1}. These averages agreed well with our full-size manikin results (0.13 and 0.20, respectively) obtained in the same manner in the same wind tunnel.

An attempt was made to compare our results obtained with the simplified torso at fixed orientations with the data found with the rotating manikin (Kenny, 1995). To make this comparison valid, the particle deposition on the filter holder was taken into account, because the experimental procedure described by Kenny for the GSP sampler stated that the filter holder was weighted together with the filter. Our study allowed us to to measure the dust on the filter holder and filter separately. If this correction is applied, the average sampling efficiency, obtained in our tests with the GSP sampling 70 μm particles, becomes about 0.18 at 50 cm s^{-1} and 0.28 at 200 cm s^{-1}. Kenny's (1995) report does not contain any data for 70 μm particles or for 200 cm s^{-1}; the results were obtained with 55, 81, and 85 μm particles at 50, 100, and 400 cm s^{-1}. Thus, to make the data comparison possible, linear interpolation was applied. At 50 cm s^{-1}, the average sampling efficiency of 0.18 found in our experiments with the simplified torso compares to 0.31, found by interpolation of Kenny's data. At 200 cm s^{-1}, the efficiency of 0.28 found in our tests falls in between Kenny's 0.29 found at 100 cm s^{-1} and 0.16 found at 400 cm s^{-1}.

Several studies have addressed the issue of the angular distribution of the aspiration efficiency in the 0 to 360° range, both for area sampling (Tsai *et al.*, 1995) and for personal sampling (Tsai *et al.*, 1996). The authors of these studies developed semi-empirical models

Table 2. Statistical results of tests for inequality of the mean sampling efficiencies obtained with the full-size versus the simplified torso

Wind velocity, ($cm\,s^{-1}$)	Sampling orientation	Torso[a]	Number of experiments	Mean sampling efficiency, $\bar{E}$	Std dev.	t-value	df	$t_{0.975}$	95% Confidence interval for[b] ($\bar{E}_{FST} - \bar{E}_{ST}$)	Is $\bar{E}_{FST}$ different from $\bar{E}_{ST}$?
50	Facing the wind	FST	3	0.270	0.025	− 2.275	4.73	2.633	[− 0.17; 0.01]	NO
		ST	4	0.350	0.024					
	90° to the wind	FST	2	0.037	0.004	2.048	1.48	8.505	[− 0.029; 0.047]	NO
		ST	3	0.028	0.002					
	180° to the wind	FST	3	0.170	0.009	− 1.132	3.66	2.902	[− 0.115; 0.051]	NO
		ST	4	0.202	0.027					
200	Facing the wind	FST	6	0.441	0.077	0.090	8.99	2.265	[− 0.14; 0.34]	NO
		ST	5	0.432	0.067					
	90° to the wind	FST	4	0.072	0.026	− 0.312	5.02	2.570	[− 0.15; 0.11]	NO
		ST	4	0.087	0.041					
	180° to the wind	FST	6	0.216	0.034	2.083	8.95	2.266	[0; 0.2]	NO
		ST	5	0.117	0.033					

[a] FST: Full-size torso; ST: Simplified torso.
[b] $\bar{E}_{FST}$: Mean aerosol sampling efficiency for FST; $\bar{E}_{ST}$: Mean aerosol sampling efficiency for ST.

for samplers under orientation-averaged conditions. The aspiration efficiency depends on the Stokes number and different non-dimensional parameters related to the sampling geometry, positioning of the sampler and the air flow regime (Vincent *et al.*, 1997). Thus, a different weighting scheme may be necessary to provide a better match between our proposed testing at only 0°, 90° and 180° and the 0° to 360° rotation measurement with a full size manikin. Our protocol perhaps could be improved by making measurements at additional angles, e.g. at 45° and 135°, though at the cost of significantly increasing the measurement time. However, measurement at other discrete angles did not seem to us to provide sufficient additional unique information to warrant their inclusion in the protocol.

An important advantage of taking data at discrete angles is the additional detail provided on the sampler efficiency. This information on sampler performance is lost when the measurements are integrated over all angles.

If accepted, the simplified torso will allow the use of a substantially smaller wind tunnel cross-section. The blockage ratio of the full-size torso in our wind tunnel was 16% while the blockage ratio of the simplified torso was only 3%. Hence, a wind tunnel having a cross-sectional area approximately 5 times smaller would yield acceptable results. Also, a smaller wind tunnel would result in a considerably smaller initial investment, as well as in lower maintenance expenses. As a result, it would encourage the development and the improvement of aerosol sampling instruments.

The air flow around a worker is variable, depending on external air flow magnitude and direction, as well as body orientation and temperature. Current efforts to simulate sampler behavior use full or half size manikins in large wind tunnels to estimate sampler efficiency. Previous researchers demonstrated that samplers placed on workers experience a different flow field and hence have a different sampling efficiency than free-standing samplers (Buchan *et al.*, 1986). The present study is an attempt to further distill the important aspects of sampling efficiency by evaluating it at three angles with respect to external air flow. It is assumed here that air flow at other angles and conditions can be simulated by a linear combination of measurements at these three angles. Furthermore, it appears that a body much smaller than a manikin can produce the external flow patterns that samplers are typically exposed to. Other issues that have been considered for incorporation into a manikin, such as breathing and heating, interact with the sampler through a change in flow direction or velocity. If the sampler on the simplified torso responds to the external flow in the same way as on the full size manikin, then we suggest that the sampler may respond in the same manner to these secondary flow effects.

CONCLUSIONS

Attempts to produce international agreement on the best approach for approval of inhalable samplers have spurred our and other researchers' (e.g. Ramachandran *et al.*, 1998) interest in a faster and less expensive approach to sampler testing. A simplified approach to testing inhalable aerosol samplers has been presented. The technique reduces variability due to body shape and breathing patterns that have been used in other test systems and allows sampling efficiency measurements at several angles simultaneously, e.g. 0°, 90°, and 180°. It is assumed here that these three angles may represent the most important flow regimes that need to be characterized for an acceptable inhalable aerosol sampler. Nevertheless, the weighting of results from the simplified body at 0°, 90°, and 180° may need to be compared in more detail to measurements using a rotating manikin. Further studies are currently being conducted in this area with different commercially available samplers and various particle sizes.

Patterns of flow approaching the samplers' inlets on the simplified test body appeared similar to those near samplers on the full-size manikin, indicating that particle trajectories are also likely to be similar in both cases. A preliminary test of the GSP sampler efficiency at 70 μm indicated that the simplified test body gave results that were not statistically different from those taken with the full-size manikin. If the proposed simplified method is used as a conventional technique for testing inhalable samplers, the between-laboratory variability

of results due to manikin shape and sampler positioning may be reduced. The wind tunnel required for the simplified test body is substantially smaller and less expensive than those currently in use for inhalable sampler testing.

Acknowledgements—The authors would like to thank Dr David Bartley of the National Institute for Occupational Safety and Health (NIOSH), Cincinnati, for the helpful discussions on the statistical approach used in this study. The authors are grateful to Dr Martin Harper of SKC Inc. for making experimental materials available.
Disclaimer—Mention of product or company name does not constitute endorsement by the Centers for Disease Control and Prevention.

REFERENCES

American Conference of Governmental Industrial Hygienists (ACGIH) (1995) *Air Sampling Instruments for Evaluation of Atmospheric Contaminants*, 8th Edition, ACGIH, Cincinnati, OH, p. 20.
American Conference of Governmental Industrial Hygienists (ACGIH) (1996) *Threshold Limit Values for Chemical Substances and Physical Agents and Biological Exposure Indices*, ACGIH, Cincinnati, OH, p. 45.
Belyaev, S. P. and Levin, L. M. (1974) Techniques for collection of representative aerosol samples. *J. Aerosol Sci.* **5,** 325–338.
Berry, R. R. and Froude, S. (1989) An investigation of wind conditions in the workplace to assess their affect on the quantity of dust inhaled. Health and Safety Executive Report, IR/L/DS/89/3, Health and Safety Executive, London, p. 26.
Buchan, R. M., Soderholm, S. C. and Tillery, M. I. (1986) Aerosol sampling efficiency of 37-mm filter cassettes. *Am. Ind. Hyg. Assoc. J.* **47,** 825–831.
Bull, R. K., Stevens, D. C. and Marshall, M. (1987) Studies of aerosol distributions in a small laboratory and around a humanoid phantom. *J. Aerosol Sci.* **3,** 321–335.
CEN (Comité Européen de Normalisation) (1993) Workplaces atmospheres: size fraction definitions for measurements of airborne particles in the workplace. CEN standard EN 481, CEN, Brussels.
CEN (Comité Européen de Normalisation) (1997) Workplace atmospheres: assessment of performance of instruments for measurement of airborne particle concentrations. CEN/TC137/WG3/N192, CEN, Brussels.
Chung, K. Y. K., Ogden, T. L. and Vaughan, N. P. (1987) Wind effects on personal dust samplers. *J. Aerosol Sci.* **18,** 159–174.
Flynn, M. R., Chen, M., Kim, T. and Muthedath, P. (1995) Computational simulation of worker exposure using a particle trajectory method. *Ann. Occup. Hyg.* **39,** 277–289.
Flynn, M. R. and Ljungqvist, B. (1995) A review of wake effects on worker exposure. *Ann. Occup. Hyg.* **39,** 211–221.
Hinds, W. C. and Kuo, T.-L. (1995) A low velocity wind tunnel to evaluate inhalability and sampler performance for large dust particles. *Appl. Occup. Environ. Hyg.* **10,** 549–556.
Ingham, D. B. and Yan, B. (1994) The effect of a cylindrical backing body on the sampling efficiency of a cylindrical sampler. *J. Aerosol Sci.* **25,** 535–541.
ISO (International Organization for Standardization) (1995) Air quality – particle size fraction definitions for health-related sampling. ISO standard 7708, ISO, Geneva.
Johnson, A. E., Flechter, B. and Saunders, C. J. (1996) Air movement around a worker in a low speed flow field. *Ann. Occup. Hyg.* **40,** 57–64.
Kennedy, E. R., Fischbach, T. J., Song, R., Eller, P. M. and Shulman, S. A. (1995) Guidelines for air sampling and analytical method development. U.S. Dept. Of Health and Human Services, Public Health Service, Centers for Disease Control and Prevention, National Institute for Occupational Safety and Health, DHHS (NIOSH) Publication No. 95-117, Cincinnati, OH.
Kenny, L. C. (1995) Pilot study of CEN protocols for the performance testing of workplace aerosol sampling instruments. Health and Safety Laboratory Report No. IR/L/DS/95/18, available from author.
Kenny, L. C., Aitken, R., Chalmers, C., Fabriès, J. F., Gonzales-Fernandez, E., Krombout, H., Lidèn, G., Mark, D., Riediger, G. and Prodi, V. (1997) A collaborative European study of personal inhalable aerosol sampler performance. *Ann. Occup. Hyg.* **41,** 135–153.
Kim, T. and Flynn, M. R. (1991) Airflow pattern around a worker in a uniform free stream. *Am. Ind. Hyg. Assoc. J.* **52,** 287–296.
Mark, D., Lyons, C. P., Upton S. L. and Kenny, L. C. (1994) Wind tunnel testing of the sampling efficiency of personal aerosol samplers. *J. Aerosol Sci.* **25,** S339–S340.
Mark, D. and Vincent, J. H. (1986) A new personal aerosol sampler for airborne total dust in workplaces. *Ann. Occup. Hyg.* **30,** 89–102.
Mark, D., Vincent, J. H., Gibson, H. and Witherspoon, W. A. (1985) Applications of closely graded powders of fused alumina as test dusts for aerosol studies. *J. Aerosol Sci.* **16,** 125–131.
Ranade, M. B., Woods, F.-L., Chen, L. J., Purdue, L. J. and Rehme, K. A. (1990) Wind tunnel evaluation of PM_{10} samplers. *Aerosol Sci. Technol.* **13,** 54–71.
Ramachandran, G., Sreenath, A. and Vincent, J. (1998) Towards a new method for experimental determination of aerosol sampler aspiration efficiency in small wind tunnels. *J. Aerosol Sci.* **29,** 875–891.
Rodes, C. E., Kamens, R. M. and Wiener, R. W. (1995) Experimental considerations for the study of contaminant dispersion near the body. *Am. Ind. Hyg. Assoc.* **56,** 535–545.
Satterthwaite, F. E. (1946) An approximate distribution of estimates of variance components. *Biometrica* **2,** 110–114.
Schlichting, H. (1979) *Boundary Layer Theory*, 7th Edition. McGraw-Hill, New York.
Smith, H. F. (1938) The problem of comparing the results of two experiments with unequal errors. *J. Council Sci. Ind. Res.* **9,** 211–212.

Sreenath, A., Ramachandran, G. and Vincent, J. H. (1997) Experimental investigation into the nature of airflows near bluff bodies with aspiration, with implications to aerosol sampling. *Atmos. Environ.* **15,** 2349–2359.
Tsai, P. J., Vincent, J. H., Mark, D. and Maldonado, G. (1995) Impaction model for the aspiration efficiencies of aerosol samplers in moving air under orientation-averaged conditions. *Aerosol Sci. Technol.* **22,** 271–286.
Tsai, P. J., Vincent, J. H. and Mark, D. (1996) Semi-empirical model for the aspiration efficiencies of personal aerosol samplers of the type widely used in occupational hygiene. *Ann. Occup. Hyg.* **40,** 93–113.
Vaughan, N. P., Milligan, B. D. and Ogden, T. L. (1989) Filter weighing reproducibility and the gravimetric detection limit. *Ann. Occup. Hyg.* **33,** 331–337.
Vincent, J. H. (1989) *Aerosol Sampling Science and Practice*. Wiley, New York, pp. 283, 328.
Vincent, J. H. and Mark, D. (1990) Entry characteristics of practical workplace aerosol samplers in relation to ISO philosophy. *Ann. Occup. Hyg.* **34,** 249–262.
Vincent, J. H., Ramachandran, G., Pui, D. Y. H., Gomes, M. S. P., Sato, S. and Sreenath, A. (1997) Experimental studies of particle transport in air flows near bluff bodies, with and without aspiration. *Proc. Amer. Soc. Mech. Engineers, Fluid Engineering Summer Meeting*, FEDSM97-3634.
Wood, J. D. and Birkett, J. L. (1979) External airflow effects on personal sampling. *Ann. Occup. Hyg.* **22,** 299–310.
Witschger, O., Wrobel, R., Fabriès, J. F., Görner, P. and Renoux, A. (1997) A new experimental wind tunnel facility for aerosol sampling investigations. *J. Aerosol Sci.* **28,** 833–851.